Journal of the Korean Nuclear Society
Volume 32, Number 4, pp.328~341, August 2000

Modal Analysis of Coaxial Shells with Fluid-Filled Annulus

Myung Jo Jhung and Yong Beum Kim
Korea Institute of Nuclear Safety
19 Kusong-dong, Yusong-gu, Taejon, 305-338, Korea
mjj@kins.re.kr

Kyeong Hoon Jeong and Suhn Choi
Korea Atomic Energy Research Institute
150 Dukjin-dong, Yusong-gu, Taejon 305-353, Korea

(Received December 28, 1999)

Abstract

Investigated in this study are the modal characteristics of the coaxial cylindrical shells with fluid-filled annulus. Theoretical method is developed to find the natural frequencies of the shell using the finite Fourier series expansion, and their results are compared with those of finite element method to verify the validation of the method developed. The effect of the fluid-filled annulus and the boundary conditions on the modal characteristics of the coaxial shells is investigated using a finite element modeling.

Key Words : cylindrical shell, modal characteristic, fluid-filled annulus, finite element method

1. Introduction

Coaxial shells or cylinders containing fluid have been widely used as structural components in various applications. One example is reactor internal structures such as core support barrel and upper structure barrel coupled with each other by fluid-filled annulus [1]. To assure the reliability of those components and to obtain information that will enable a designer to predict plant vibration amplitude during normal operations of a nuclear power plant [2], it is necessary to investigate extensively flow-induced vibration, necessitating the investigation of the modal characteristics.

Several previous investigations have been performed to analyze the free vibration of fluid-filled, coaxial cylindrical shells [3, 4]. However, previous theories were limited to the approximated methods and could provide only the in-phase and out-of-phase modes of coaxial shells with small annular fluid gap compared to the shell diameters. Therefore, they can only be applicable to the low axial and circumferential modes of coaxial shells with small annular fluid gap. Practically, there exist many ambiguous vibrational modes in addition to the in-phase and out-of-phase modes.

This study develops an advanced general theory

to calculate the natural frequencies for all vibrational modes of two coaxial circular cylindrical shells coupled with fluid. To support the validity of the proposed theory, finite element analyses are carried out for various boundary conditions. Also it has been shown analytically and experimentally that the immersion of a body in a dense fluid medium lowers its natural frequency and significantly alters its vibratory response as compared to that in air [5, 6]. Therefore the effect of the inclusion of the fluid-filled annulus on the natural frequencies of the coaxial shells is investigated by comparing frequencies between shells with and without fluid-filled annulus. The effect is also addressed with respect to the boundary conditions at both ends of coaxial shells.

2. Theory

2.1. Equation of Motion

Consider fluid-filled coaxial cylindrical shells with clamped boundary conditions at both ends. The cylindrical shells have mean radii R_1, and R_2, height L, and wall thickness h, as shown in Figure 1. The Sanders' shell equations [7] as the governing equations for both shells where the hydrodynamic effects are considered, can be written as :

$$R_j^2 u_{j,xx}+\frac{(1-\mu)}{2}\left(1+\frac{k_j}{4}\right)u_{j,\theta\theta}+R_j\left\{\frac{(1+\mu)}{2}-\frac{3(1-\mu)}{8}k_j\right\}v_{j,x\theta}+\mu R_j w_{j,x} + \frac{(1-\mu)}{2}R_j k_j w_{j,x\theta\theta}=\frac{\rho R_j^2(1-\mu^2)}{E}u_{j,tt} \tag{1a}$$

$$R_j\left\{\frac{(1+\mu)}{2}-\frac{3(1-\mu)}{8}k_j\right\}u_{j,x\theta}+(1+k_j)v_{j,\theta\theta}+\frac{(1-\mu)}{2}R_j^2\left(1+\frac{9k_j}{4}\right)v_{j,xx} - \frac{(3-\mu)}{2}R_j^2 k_j w_{j,xx\theta}+w_{j,\theta}-k_j w_{j,\theta\theta\theta}=\frac{\rho R_j^2(1-\mu^2)}{E}v_{j,tt}, \tag{1b}$$

$$R_j\left\{\frac{(1+\mu)}{2}-\frac{3(1-\mu)}{8}k_j\right\}u_{j,x\theta}+(1+k_j)v_{j,\theta\theta}+\frac{(1-\mu)}{2}R_j^2\left(1+\frac{9k_j}{4}\right)v_{j,xx} - \frac{(3-\mu)}{2}R_j^2 k_j w_{j,xx\theta}+w_{j,\theta}-k_j w_{j,\theta\theta\theta}=\frac{\rho R_j^2(1-\mu^2)}{E}v_{j,tt}, \tag{1c}$$

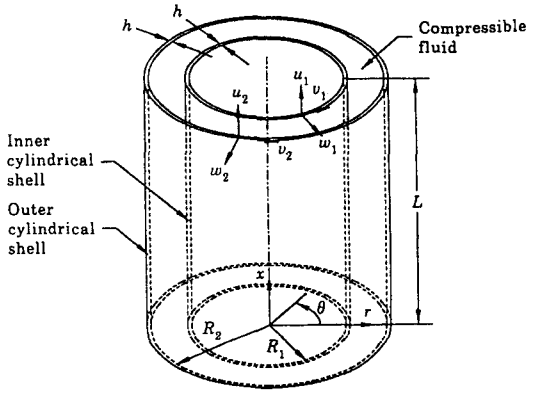

Fig. 1. Coaxial Cylindrical Shells with Fluid-filled Annulus

where k_j is $h^2/12R_j^2$, μ Poisson' s ratio, t time, p_j dynamic liquid pressure and u_j, v_j, w_j, axial, tangential, radial dynamic displacements of shells, respectively. Also, subscripts 1 and 2 represent the inner and outer shells, and comma (,) in the equations denotes a partial derivative with respect to the corresponding variable. For a complete description of the shell motions, it is necessary to add boundary conditions to the equations of motion. Consider the simplest end arrangements of the shell on the top and bottom supports. At both ends of concentrically arranged shells, the boundary conditions will obviously hold:

for the bottom support of the inner shell,

$$M_{x1}(0) = N_{x1}(0) = v_1(0) = w_1(0) = 0, \tag{2a}$$

for the top support of the inner shell,

$$Mx1(L) = Nx1(L) = v1(L) = w1(L) = 0, \tag{2b}$$

for the bottom support of the outer shell,

$$M_{x2}(0) = N_{x2}(0) = v_2(0) = w_2(0) = 0, \tag{2c}$$

for the top support of the outer shell,

$$M_{x2}(L) = N_{x2}(L) = v_2(L) = w_2(L) = 0, \tag{2d}$$

where M_{xj} and N_{xj} denote the bending moment

and the membrane tensile force, respectively. All geometric boundary conditions applicable to the ends of the shells can be reduced to the following equations :

for the clamped-clamped condition,

$$v_1(0) = w_1(0) = v_2(0) = w_2(0) = 0, \quad (3a)$$

$$v_1(L) = w_1(L) = v_2(L) = w_2(L) = 0, \quad (3b)$$

for the clamped-free condition,

$$v_1(0) = w_1(0) = v_2(0) = w_2(0) = 0, \quad (3c)$$

$$N_{x1}(L) = M_{x1}(L) = N_{x2}(L) = M_{x2}(L) = 0, \quad (3d)$$

for the simply supported-simply supported condition,

$$v_1(0) = w_1(0) = v_2(0) = w_2(0) = 0, \quad (3e)$$

$$M_{x1}(L) = M_{x2}(L) = 0. \quad (3f)$$

The relationships between the boundary forces and displacements are

$$N_{xj} = \frac{Eh}{1-\mu^2}\left[u_{j,x} + \frac{\mu}{R_j}v_{j,\theta} + \frac{\mu}{R_j}w_j\right], \quad (4a)$$

$$N_{x\theta j} = \frac{Eh}{2(1+\mu)}\left[\frac{1}{R_j}\left(1-\frac{3}{4}k_j\right)u_{j,\theta} + \left(1+\frac{9}{4}k_j\right)v_{j,x} - 3k_j w_{j,x\theta}\right], \quad (4b)$$

$$Q_{xj} = \frac{Eh^3}{12(1-\mu^2)}\left[-\frac{(1-\mu)}{2R_j^3}u_{j,\theta\theta} + \frac{(3-\mu)}{2R_j^2}v_{j,x\theta} - \frac{(2-\mu)}{R_j^2}w_{j,x\theta\theta} - w_{j,xxx}\right], \quad (4c)$$

$$M_{xj} = \frac{Eh^3}{12(1-\mu^2)}\left[\frac{\mu}{R_j^2}\left(v_{j,\theta} - w_{j,\theta\theta}\right) - w_{j,xx}\right]. \quad (4d)$$

$N_{x\theta j}$ and Q_{xj} denote the membrane shear force and transverse shear force per unit length, respectively.

2.2. Modal Functions

A general relation for the dynamic displacements in any vibration mode of the shell can be written in the following form for the cylindrical coordinate r, θ.

$$\begin{bmatrix} u_j(x,\theta,t) \\ v_j(x,\theta,t) \\ w_j(x,\theta,t) \end{bmatrix} = \begin{bmatrix} u_j(x,\theta) \\ v_j(x,\theta) \\ w_j(x,\theta) \end{bmatrix} \exp(i\omega t), \quad j=1,2. \quad (5)$$

where $u_j(x,\theta)$, $v_j(x,\theta)$ and $w_j(x,\theta)$ are modal functions corresponding to the axial, tangential and radial displacements, respectively. These modal functions along the axial direction can be described by a sum of linear combinations of the Fourier series that are orthogonal.

$$\begin{bmatrix} u_j(x,\theta) \\ v_j(x,\theta) \\ w_j(x,\theta) \end{bmatrix} = \begin{bmatrix} \sum_{n=1}^{\infty}\sum_{m=1}^{\infty} A_{mnj}\sin\left(\frac{m\pi x}{L}\right)\cos n\theta \\ \sum_{n=1}^{\infty}\left\{B_{onj} + \sum_{m=1}^{\infty} B_{mnj}\cos\left(\frac{m\pi x}{L}\right)\right\}\sin n\theta \\ \sum_{n=1}^{\infty}\left\{C_{onj} + \sum_{m=1}^{\infty} C_{mnj}\cos\left(\frac{m\pi x}{L}\right)\right\}\cos n\theta \end{bmatrix} \quad (6)$$

The derivatives of the above modal functions for the shell can be obtained using the finite Fourier transformation [8]. The modal functions and their derivatives of the cylindrical shell were described in reference [7].

2.3. Equation of Fluid Motion

The inviscid, irrotational and compressible fluid movement due to shell vibration is described by the Helmholz equation :

$$\Phi_{,rr} + \frac{1}{r}\Phi_{,r} + \frac{1}{r^2}\Phi_{,\theta\theta} + \Phi_{,xx} = \frac{1}{c^2}\Phi_{,tt}, \quad (7)$$

where c is the speed of sound in the fluid medium equal to $\sqrt{B/\rho_o}$, B is the bulk modulus of elasticity of fluid and ρ_o stands for the fluid density. It is possible to separate the function Φ with respect to x by observing that, in the axial direction, the rigid surfaces support the edges of the shells;

thus

$$\Phi(x,r,\theta,t)=i\omega\phi(r,\theta,x)\exp(i\omega t)$$
$$=i\omega\eta(r,\theta)f(x)\exp(i\omega t), \quad (8)$$

where ω is the fluid-coupled frequency of the shells and $i = \sqrt{-1}$. Substitution of equation (8) into the partial differential equation (7) gives

$$\frac{\eta(r,\theta),_{rr}+\frac{1}{r}\eta(r,\theta),_{r}+\frac{1}{r^2}\eta(r,\theta),_{\theta\theta}+\left(\frac{\omega}{c}\right)^2\eta(r,\theta)}{\eta(r,\theta)} \quad (9)$$
$$=-\frac{f(x),_{xx}}{f(x)}=\left(\frac{m\pi}{L}\right)^2.$$

It is possible to solve the partial differential equation (9) by the separation of the variables. The solution can be obtained with respect to the cylindrical coordinates, r, θ and x.

for $\frac{m\pi}{L}\geq\frac{\omega}{c}$,

$$\phi(r,\theta,x)=\sum_{n=1}^{\infty}\left[\begin{array}{c} D_{on1}J_n\left(\frac{\omega r}{c}\right)+D_{on2}Y_n\left(\frac{\omega r}{c}\right) \\ +\sum_{m=1}^{\infty}\{D_{mn1}I_n(\alpha_{mn}r)+F_{mn2}K_n(\alpha_{mn}r)\}\cos\left(\frac{m\pi x}{L}\right)\end{array}\right]\cos n\theta \quad (10a)$$

and for $\frac{m\pi}{L}<\frac{\omega}{c}$,

$$\phi(r,\theta,x)=\sum_{n=1}^{\infty}\left[\begin{array}{c} D_{on1}J_n\left(\frac{\omega r}{c}\right)+D_{on2}Y_n\left(\frac{\omega r}{c}\right) \\ +\sum_{m=1}^{\infty}\{D_{mn1}J_n(\alpha_{mn}r)+F_{mn2}Y_n(\alpha_{mn}r)\}\cos\left(\frac{m\pi x}{L}\right)\end{array}\right]\cos n\theta \quad (10b)$$

where J_n and Y_n are Bessel functions of the first and second kinds of order n, whereas I_n and K_n are modified Bessel functions of the first and second kinds of order n. ϕ means the spatial velocity potential of the contained compressible fluid and α_{mn} is related to the speed of sound in the fluid medium as ;

$$\alpha_{mn}=\sqrt{\left|\left(\frac{m\pi}{L}\right)^2-\left(\frac{\omega}{c}\right)^2\right|} \quad \text{for } m=1,2,3,.... \quad (11)$$

The boundary conditions of the velocity potential ϕ appear as follows;

(a) impermeable rigid surfaces on the bottom is

$$\left.\frac{\partial\phi(x,\theta,r)}{\partial x}\right|_{x=0}=0; \quad (12)$$

(b) as there exists no free surface, the axial fluid velocity at the rigid top is also zero, so

$$\left.\frac{\partial\phi(x,\theta,r)}{\partial x}\right|_{x=L}=0; \quad (13)$$

(c) the radial fluid velocity along the outer wetted surface of the inner shell must be identical to the radial velocity of the flexible shell, so

$$\left.\frac{\partial\phi(x,\theta,r)}{\partial r}\right|_{r=R_1}=w_1(x,\theta); \quad (14)$$

(d) the radial fluid velocity along the inner wetted surface of the outer shell must be identical to the radial velocity of the shell, so

$$\left.\frac{\partial\phi(x,\theta,r)}{\partial r}\right|_{r=R_2}=-w_2(x,\theta). \quad (15)$$

Substitution of equations (6), (10a) and (10b) into equations (14) and (15) gives the relationships :

for $m\pi/L\geq\omega/c$,

$$\sum_{n=1}^{\infty}\left[\begin{array}{c}\left(\frac{\omega}{c}\right)\left\{D_{on1}J_n'\left(\frac{\omega R_1}{c}\right)+D_{on2}Y_n'\left(\frac{\omega R_1}{c}\right)\right\} \\ +\sum_{m=1}^{\infty}\alpha_{mn}\{D_{mn1}I_n'(\alpha_{mn}R_1)+D_{mn2}K_n'(\alpha_{mn}R_1)\}\cos\left(\frac{m\pi x}{L}\right)\end{array}\right]\cos n\theta \quad (16a)$$
$$=\sum_{n=1}^{\infty}\left[C_{on1}+\sum_{m=1}^{\infty}C_{mn1}\cos\left(\frac{m\pi x}{L}\right)\right]\cos n\theta,$$

for $m\pi/L<\omega/c$,

$$\sum_{n=1}^{\infty}\left[\begin{array}{c}\left(\frac{\omega}{c}\right)\left\{D_{on1}J_n'\left(\frac{\omega R_2}{c}\right)+D_{on2}Y_n'\left(\frac{\omega R_2}{c}\right)\right\} \\ +\sum_{m=1}^{\infty}\alpha_{mn}\{D_{mn1}I_n'(\alpha_{mn}R)+D_{mn2}K_n'(\alpha_{mn}R_2)\}\cos\left(\frac{m\pi x}{L}\right)\end{array}\right]\cos n\theta \quad (16b)$$
$$=-\sum_{n=1}^{\infty}\left[C_{on2}+\sum_{m=1}^{\infty}C_{mn2}\cos\left(\frac{m\pi x}{L}\right)\right]\cos n\theta.$$

Now, equation (16) will be reduced to

$$\left(\frac{\omega}{c}\right)\begin{bmatrix}J_n'\left(\frac{\omega}{c}R_1\right) & Y_n'\left(\frac{\omega}{c}R_1\right)\\ J_n'\left(\frac{\omega}{c}R_2\right) & Y_n'\left(\frac{\omega}{c}R_2\right)\end{bmatrix}\begin{Bmatrix}D_{on1}\\ D_{on2}\end{Bmatrix}=\begin{Bmatrix}C_{on1}\\ -C_{on2}\end{Bmatrix}, \quad (17a)$$

$$\alpha_{mn}\begin{bmatrix} I_n'(\alpha_{mn}R_1) & K_n'(\alpha_{mn}R_1) \\ I_n'(\alpha_{mn}R_2) & K_n'(\alpha_{mn}R_2) \end{bmatrix}\begin{Bmatrix} D_{mn1} \\ D_{mn2} \end{Bmatrix} = \begin{Bmatrix} C_{mn1} \\ -C_{mn2} \end{Bmatrix}, \quad (17b)$$

When $m\pi/L < \omega/c$, $I_n'(\ )$ and $K_n'(\ )$ in equations (16a), (16b) and (17b) should be replaced by $J_n'(\ )$ and $Y_n'(\ )$, respectively. When the hydrostatic pressures on the shells are neglected, the hydrodynamic pressures along the inner and outer wetted shell surfaces can be given by

$$p_j(x,\theta,t) = \delta_j \rho_o \omega^2 \phi(x,\theta,R_j)\exp(i\omega t), \quad (18)$$

where $\delta_j = 1$ for $j = 1$ and $\delta_j = -1$ for $j = 2$. Finally the hydrodynamic forces on the inner and outer shells can be written as

$$\frac{R_j^2 p_j(x,\theta,t)}{D} = \frac{\rho_o \omega^2 R_j^2 \delta_j}{D}\sum_{n=1}^{\infty}\Big\{C_{on1}\Gamma_{onj} + C_{on2}G_{onj} + \sum_{m=1}^{\infty}\left[C_{mn1}\Gamma_{mnj} + C_{mn2}G_{mnj}\right]\cos\left(\frac{m\pi x}{L}\right)\Big\}\cos n\theta\exp(i\omega t) \quad (19)$$

2.4. General Formulation

The dynamic displacements and their derivatives can be represented by a Fourier sine and cosine series in an open range of $0 < x < L$ and with the end values using the finite Fourier transformation [7]. Substitution of the displacements and their derivatives into the governing Sanders' shell equation (1a), (1b) and (1c), leads to an explicit relation for B_{onj}, C_{onj} and a set of equations for A_{mnj}, B_{mnj}, C_{mnj} as follows ;

$$\begin{bmatrix} B_{onj} \\ C_{onj} \end{bmatrix} = \begin{bmatrix} q_{1j} & q_{2j} & q_{3j} & q_{4j} \\ q_{5j} & q_{6j} & q_{7j} & q_{8j} \end{bmatrix}\begin{bmatrix} u_j^{\circ} + u_j^{L} \\ \tilde{v}_j^{\circ} + \tilde{v}_j^{L} \\ \tilde{w}_j^{\circ} + \tilde{w}_j^{L} \\ \tilde{\tilde{w}}_j^{\circ} + \tilde{\tilde{w}}_j^{L} \end{bmatrix}, \quad (20)$$

$$\begin{bmatrix} d_{11} & d_{12} & d_{13} & 0 & 0 & 0 \\ d_{12} & d_{22} & d_{23} & 0 & 0 & 0 \\ d_{13} & d_{23} & d_{33} & 0 & 0 & d_{63} \\ 0 & 0 & 0 & d_{44} & d_{45} & d_{46} \\ 0 & 0 & 0 & d_{45} & d_{55} & d_{56} \\ 0 & 0 & d_{36} & d_{46} & d_{56} & d_{66} \end{bmatrix}\begin{bmatrix} A_{mn1} \\ B_{mn1} \\ C_{mn1} \\ A_{mn2} \\ B_{mn2} \\ C_{mn2} \end{bmatrix}$$

$$= \begin{bmatrix} -a_{11}m[u_1^{\circ} + (-1)^m u_1^{L}] \\ a_{12}[u_1^{\circ} + (-1)^m u_1^{L}] + a_{13}[\tilde{v}_1^{\circ} + (-1)^m \tilde{v}_1^{L}] + a_{14}[\tilde{w}_1^{\circ} + (-1)^m \tilde{w}_1^{L}] \\ a_{15}[u_1^{\circ} + (-1)^m u_1^{L}] + a_{14}[\tilde{v}_1^{\circ} + (-1)^m \tilde{v}_1^{L}] + a_{18}[\tilde{w}_1^{\circ} + (-1)^m \tilde{w}_1^{L}] \\ -a_{21}m[u_2^{\circ} + (-1)^m u_2^{L}] \\ a_{22}[u_2^{\circ} + (-1)^m u_2^{L}] + a_{23}[\tilde{v}_2^{\circ} + (-1)^m \tilde{v}_2^{L}] + a_{24}[\tilde{w}_2^{\circ} + (-1)^m \tilde{w}_2^{L}] \\ a_{25}[u_2^{\circ} + (-1)^m u_2^{L}] + a_{24}[\tilde{v}_2^{\circ} + (-1)^m \tilde{v}_2^{L}] + a_{28}[\tilde{w}_2^{\circ} + (-1)^m \tilde{w}_2^{L}] \end{bmatrix} \quad (21)$$

$$\begin{bmatrix} +0 \\ +0 \\ +a_{19}[\tilde{\tilde{w}}_1^{\circ} + (-1)^m \tilde{\tilde{w}}_1^{L} - m^2\tilde{w}_1^{\circ} - m^2(-1)^m \tilde{w}_1^{L}] \\ +0 \\ +0 \\ +a_{29}[\tilde{\tilde{w}}_2^{\circ} + (-1)^m \tilde{\tilde{w}}_2^{L} - m^2\tilde{w}_2^{\circ} - m^2(-1)^m \tilde{w}_2^{L}] \end{bmatrix}$$

where the end values u_j°, u_j^{L}, $\tilde{v}_j^{\circ}$, $\tilde{v}_j^{L}$, $\tilde{w}_j^{\circ}$, $\tilde{w}_j^{L}$, $\tilde{\tilde{w}}_j^{\circ}$ and $\tilde{\tilde{w}}_j^{L}$ in equations (20) and (21) are defined as ;

$$u_j^{\circ} = -\frac{2u_j(0,\theta)}{\pi\cos n\theta}, \quad u_j^{L} = \frac{2u_j(L,\theta)}{\pi\cos n\theta},$$

$$\tilde{v}_j^{\circ} = -\frac{2Lv_{j,x}(0,\theta)}{\pi^2\sin n\theta}, \quad \tilde{v}_j^{L} = \frac{2Lv_{j,x}(L,\theta)}{\pi^2\sin n\theta},$$

$$\tilde{w}_j^{\circ} = -\frac{2Lw_{j,x}(0,\theta)}{\pi^2\cos n\theta}, \quad \tilde{w}_j^{L} = \frac{2Lw_{j,x}(L,\theta)}{\pi^2\cos n\theta}, \quad (22)$$

$$\tilde{\tilde{w}}_j^{\circ} = -\frac{2L^3w_{j,xxx}(0,\theta)}{\pi^4\cos n\theta}, \quad \tilde{\tilde{w}}_j^{L} = \frac{2L^3w_{j,xxx}(L,\theta)}{\pi^4\cos n\theta}$$

The equivalent hydrodynamic mass effect on the inner and outer shell is included in the coefficient d_{33} and d_{66}, respectively. The coefficient d_{36} indicates the equivalent hydraulic pressure on the inner shell induced by the outer shell motion, and similarly d_{63} stands for the equivalent hydraulic pressure on the outer shell induced by the inner shell motion. Generally speaking, the coefficient $d_{36} \neq d_{63}$. Therefore the matrix equation (21) is asymmeric and is coupled by two coefficient terms d_{36} and d_{63}.

The forces and at the ends of the shells can be

written as a combination of some boundary values of displacement and their derivatives using equation (3). The boundary values of displacement and their derivatives, $\widetilde{v}_j^o$, $\widetilde{v}_j^L$, $\widetilde{\widetilde{w}}_j^o$ and $\widetilde{\widetilde{w}}_j^L$ can be transformed in a combination of the boundary values of u_j, $\widetilde{w}_j$, $N_{x\theta j}$ and Q_{xj} by equation (4), as written in the form

$$\begin{bmatrix} \widetilde{v}_j^o \\ \widetilde{v}_j^L \\ \widetilde{\widetilde{w}}_j^o \\ \widetilde{\widetilde{w}}_j^L \end{bmatrix} = \begin{bmatrix} u_j^o & \widetilde{w}_j^o & N_{x\theta}^o & 0 & 0 & 0 & 0 \\ u_j^L & \widetilde{w}_j^L & N_{x\theta}^L & 0 & 0 & 0 & 0 \\ 0 & 0 & 0 & u_j^o & \widetilde{w}_j^o & N_{x\theta}^o & Q_{xj}^o \\ 0 & 0 & 0 & u_j^L & \widetilde{w}_j^L & N_{x\theta}^L & Q_{xj}^L \end{bmatrix} \begin{bmatrix} g_{1j} \\ g_{2j} \\ g_{3j} \\ g_{4j} \\ g_{5j} \\ g_{6j} \\ g_{7j} \end{bmatrix} \tag{23}$$

where

$$\begin{bmatrix} N_{x\theta}^o \\ N_{x\theta}^L \\ Q_{xj}^o \\ Q_{xj}^L \end{bmatrix} = \begin{bmatrix} \frac{1}{\sin n\theta} & 0 & 0 & 0 \\ 0 & -\frac{1}{\sin n\theta} & 0 & 0 \\ 0 & 0 & \frac{1}{\cos n\theta} & 0 \\ 0 & & 0 & -\frac{1}{\cos n\theta} \end{bmatrix} \begin{bmatrix} N_{x\theta}(0,\theta) \\ N_{x\theta}(L,\theta) \\ Q_{xj}(0,\theta) \\ Q_{xj}(L,\theta) \end{bmatrix} \tag{24}$$

Substituting equation (23) into equations (20) and (21) gives

$$\begin{bmatrix} B_{on1} \\ B_{on2} \\ C_{on1} \\ C_{on2} \end{bmatrix} = \sum_{j=1}^{2} \begin{bmatrix} \beta_{1j} & \beta_{2j} & \beta_{3j} & \beta_{4j} \\ \beta_{5j} & \beta_{6j} & \beta_{7j} & \beta_{8j} \\ \delta_{1j} & \delta_{2j} & \delta_{3j} & \delta_{4j} \\ \delta_{5j} & \delta_{6j} & \delta_{7j} & \delta_{8j} \end{bmatrix} \begin{bmatrix} u_j^o + u_j^L \\ \widetilde{w}_j^o + \widetilde{w}_j^L \\ N_{x\theta}^o + N_{x\theta}^L \\ Q_{xj}^o + Q_{xj}^L \end{bmatrix} \tag{25}$$

$$\begin{bmatrix} A_{mn1} \\ B_{mn1} \\ C_{mn1} \\ A_{mn2} \\ B_{mn2} \\ C_{mn2} \end{bmatrix} = [\zeta] \begin{bmatrix} u_1^o + (-1)^m u_1^L \\ u_2^o + (-1)^m u_2^L \\ \widetilde{w}_1^o + (-1)^m \widetilde{w}_1^L \\ \widetilde{w}_2^o + (-1)^m \widetilde{w}_2^L \\ N_{x\theta 1}^o + (-1)^m N_{x\theta 1}^L \\ N_{x\theta 2}^o + (-1)^m N_{x\theta 2}^L \\ Q_{x1}^o + (-1)^m Q_{x1}^L \\ Q_{x2}^o + (-1)^m Q_{x2}^L \end{bmatrix}, \tag{26}$$

where β_{ij} and δ_{ij} in equation (25) are the derived coefficients, and $[\zeta]$ is a 8×6 derived coefficients matrix. Eventually, all Fourier coefficients A_{mnj}, B_{mnj} and C_{mnj} are rearranged with a combination of the end point values as shown in equation (26).

The geometric boundary conditions that must be satisfied are associated with displacements v_j and w_j. Hence, it follows that

$$v_1(0) = \sum_{n=1}^{\infty} \left[B_{on1} + \sum_{m=1}^{\infty} B_{mn1} \right] = 0, \tag{27a}$$

$$v_1(L) = \sum_{n=1}^{\infty} \left[B_{on1} + \sum_{m=1}^{\infty} B_{mn1}(-1)^m \right] = 0, \tag{27b}$$

$$v_2(0) = \sum_{n=1}^{\infty} \left[B_{on2} + \sum_{m=1}^{\infty} B_{mn2} \right] = 0, \tag{27c}$$

$$v_2(L) = \sum_{n=1}^{\infty} \left[B_{on2} + \sum_{m=1}^{\infty} B_{mn2}(-1)^m \right] = 0, \tag{27d}$$

$$w_1(0) = \sum_{n=1}^{\infty} \left[C_{on1} + \sum_{m=1}^{\infty} C_{mn1} \right] = 0, \tag{27e}$$

$$w_1(L) = \sum_{n=1}^{\infty} \left[C_{on1} + \sum_{m=1}^{\infty} C_{mn1}(-1)^m \right] = 0, \tag{27f}$$

$$w_2(0) = \sum_{n=1}^{\infty} \left[C_{on2} + \sum_{m=1}^{\infty} C_{mn2} \right] = 0, \tag{27g}$$

$$w_2(L) = \sum_{n=1}^{\infty} \left[C_{on2} + \sum_{m=1}^{\infty} C_{mn2}(-1)^m \right] = 0. \tag{27h}$$

On the other hand, the natural boundary conditions that must be satisfied are associated with M_{xj} and N_{xj}.

$$N_{x1}(0) = \left(\frac{\pi}{L}\right)\left(\frac{u_1^o + u_1^L}{2}\right) + \left(\frac{\mu}{R_1}\right)(n B_{on1} + C_{on1}) + \sum_{m=1}^{\infty} \left[\left(\frac{\pi}{L}\right)\left(u_1^o + (-1)^m u_1^L + m A_{mn1}\right) + \left(\frac{\mu}{R_1}\right)(n B_{mn1} + C_{mn1}) \right] = 0, \tag{28a}$$

$$N_{x1}(0) = \left(\frac{\pi}{L}\right)\left(\frac{u_1^o + u_1^L}{2}\right) + \left(\frac{\mu}{R_1}\right)(n B_{on1} + C_{on1}) + \sum_{m=1}^{\infty} \left[\left(\frac{\pi}{L}\right)\left(u_1^o + (-1)^m u_1^L + m A_{mn1}\right) + \left(\frac{\mu}{R_1}\right)(n B_{mn1} + C_{mn1}) \right] = 0, \tag{28b}$$

$$N_{x1}(L)=\left(\frac{\pi}{L}\right)\left(\frac{u_1^o+u_1^L}{2}\right)+\left(\frac{\mu}{R_1}\right)\left(nB_{on1}+C_{on1}\right)$$
$$+\sum_{m=1}^{\infty}\left[\left(\frac{\pi}{L}\right)\left(u_1^o+(-1)^m u_1^L+mA_{mn1}\right)+\left(\frac{\mu}{R_1}\right)\left(nB_{mn1}+C_{mn1}\right)\right](-1)^m=0, \quad (28c)$$

$$N_{x2}(L)=\left(\frac{\pi}{L}\right)\left(\frac{u_2^o+u_2^L}{2}\right)+\left(\frac{\mu}{R_2}\right)\left(nB_{on2}+C_{on2}\right)$$
$$+\sum_{m=1}^{\infty}\left[\left(\frac{\pi}{L}\right)\left(u_2^o+(-1)^m u_2^L+mA_{mn2}\right)+\left(\frac{\mu}{R_2}\right)\left(nB_{mn2}+C_{mn2}\right)\right](-1)^m=0, \quad (28d)$$

$$M_{x1}(0)=-\left(\frac{\pi}{L}\right)^2\left(\frac{\tilde{w}_1^o+\tilde{w}_1^L}{2}\right)+\left(\frac{\mu}{R_1^2}\right)n\left(B_{on1}+nC_{on1}\right)$$
$$+\sum_{m=1}^{\infty}\left[-\left(\frac{\pi}{L}\right)^2\left(\tilde{w}_1^o+(-1)^m\tilde{w}_1^L-m^2C_{mn1}\right)+\left(\frac{\mu}{R_1^2}\right)n\left(B_{mn1}+nC_{mn1}\right)\right]=0, \quad (28e)$$

$$M_{x2}(0)=-\left(\frac{\pi}{L}\right)^2\left(\frac{\tilde{w}_2^o+\tilde{w}_2^L}{2}\right)+\left(\frac{\mu}{R_2^2}\right)n\left(B_{on2}+nC_{on2}\right)$$
$$+\sum_{m=1}^{\infty}\left[-\left(\frac{\pi}{L}\right)^2\left(\tilde{w}_2^o+(-1)^m\tilde{w}_2^L-m^2C_{mn2}\right)+\left(\frac{\mu}{R_2^2}\right)n\left(B_{mn2}+nC_{mn2}\right)\right]=0, \quad (28f)$$

$$M_{x1}(L)=-\left(\frac{\pi}{L}\right)^2\left(\frac{\tilde{w}_1^o+\tilde{w}_1^L}{2}\right)+\left(\frac{\mu}{R_1^2}\right)n\left(B_{on1}+nC_{on1}\right)$$
$$-\sum_{m=1}^{\infty}\left[\left(\frac{\pi}{L}\right)^2\left(\tilde{w}_1^o+(-1)^m\tilde{w}_1^L-m^2C_{mn1}\right)-\left(\frac{\mu}{R_1^2}\right)n\left(B_{mn1}+nC_{mn1}\right)\right](-1)^m=0, \quad (28g)$$

$$M_{x2}(L)=-\left(\frac{\pi}{L}\right)^2\left(\frac{\tilde{w}_2^o+\tilde{w}_2^L}{2}\right)+\left(\frac{\mu}{R_2^2}\right)n\left(B_{on2}+nC_{on2}\right)$$
$$-\sum_{m=1}^{\infty}\left[\left(\frac{\pi}{L}\right)^2\left(\tilde{w}_2^o+(-1)^m\tilde{w}_2^L-m^2C_{mn2}\right)-\left(\frac{\mu}{R_2^2}\right)n\left(B_{mn2}+nC_{mn2}\right)\right](-1)^m=0. \quad (28h)$$

Substitution of equations (25) and (26) for the coefficients, B_{onj}, C_{onj}, B_{mnj} and C_{mnj} into the eight constraint conditions which came from the geometric and natural boundary conditions, written as equations (27) and (28), leads to the homogeneous matrix equation ;

$$[\mathbf{E}][\mathbf{H}]=\{\mathbf{0}\}, \quad (29)$$

where [**E**] is the 16 x 16 matrix derived from equations (27) and (28), and

$$[\mathbf{H}]=\left[u_1^o \;\; u_1^L \;\; u_2^o \;\; u_2^L \;\; \tilde{w}_1^o \;\; \tilde{w}_1^L \;\; \tilde{w}_2^o \;\; \tilde{w}_2^L \;\; N_{x\theta 1}^o \;\; N_{x\theta 1}^L \;\; N_{x\theta 2}^o \;\; N_{x\theta 2}^L \;\; Q_{x1}^o \;\; Q_{x1}^L \;\; Q_{x2}^o \;\; Q_{x2}^L\right]^T. \quad (30)$$

When the cylindrical shells are clamped at both ends, the associated boundary conditions are written by equations (3a) and (3b). Hence the geometric boundary conditions expressed by equations (27a) - (27h) must be satisfied. However, $u_1 = 0$, $u_2 = 0$, $\tilde{w}_1 = 0$ and $\tilde{w}_2 = 0$ at $x = 0$ and $x = L$ are automatically satisfied by equation (5), the modal functions set. Therefore from the first, to the eighth rows of the matrix in equation (29) are enforced and the terms associated with u_j^o, u_j^L, $\tilde{w}_j^o$, and $\tilde{w}_j^L$ are released. The 8×8 frequency determinant is obtained from equations (29) by retaining the rows and columns associated with $N_{x\theta j}^o$, $N_{x\theta j}^L$, Q_{xj}^o and Q_{xj}^L. For the clamped boundary condition, the coupled natural frequencies are numerically obtained from the frequency determinant.

For the clamped-free boundary conditions, the associated boundary conditions are written by equations (3c), (3d). Hence the geometric and natural boundary conditions of equations (27a), (27c), (27e), (27g), (28c), (28d), (28g) and (28h) must be satisfied. However, $u_1 = 0$, $u_2 = 0$, $\tilde{w}_1 = 0$ and $\tilde{w}_2 = 0$ at $x = 0$ and $N_{x\theta 1}^L = N_{x\theta 2}^L = 0$, $Q_{x1}^L = Q_{x2}^L = 0$ at $x = L$ are automatically satisfied. Therefore the 1st, 3rd, 5th, 7th, 11th, 12th, 15th and 16th rows of the matrix in equation (29) are enforced and the terms associated with u_j^o, $\tilde{w}_j^o$, $N_{x\theta j}^L$, and Q_{xj}^L are released. The 8×8 frequency determinant is obtained from equations (29) by retaining the rows and columns associated with, u_j^L, $\tilde{w}_j^L$, $N_{x\theta j}^o$, and Q_{xj}^o. For the clamped-free boundary condition, the coupled natural frequencies are numerically obtained from the frequency determinant. For the simply supported case, the frequency determinant can be easily obtained by similar method.

3. Analysis

3.1. Theoretical Analysis

On the basis of the preceding analysis, the frequency determinant is numerically solved for the clamped boundary condition in order to find the natural frequencies of the coaxial circular cylindrical shells with a bounded compressible fluid. The inner and outer shells are coupled with a fluid-filled annular gap. The inner cylindrical shell has a mean radius of 100 mm, a length of 300 mm, and a wall thickness of 2 mm. The outer cylindrical shell has a mean radius of 150 mm with

Table 1. Dimensions and Material Properties

	Unit	Shell		Fluid
		Inner	*Outer*	
Length	m	0.300	0.300	
Mean radius	m	0.100	0.150	
Thickness	m	0.002	0.002	
Young' s modulus	Pa	69E9	69E9	
Poisson' s ratio		0.3	0.3	
Density	kg/m^3	2700	2700	1000
Sound speed	m/sec			1483

Table 2. Coupled Natural Frequencies of the Fluid-filled Coaxial Shells(out-of-phase/in-phase)

Circumferential mode *n*	Axial mode *m'*	Frequency (Hz)		Discrepancy		
		Theory	FEM	%	RMS	Crest Factor
1	1	391/1737	405/1794	3.5/3.2	5.3/3.2	1.4/1.0
	2	848/	916/	7.4/		
	3	1398/	1398/	0.0/		
	4	1909/	2044/	6.6/		
2	1	436/997	436/1002	0.0/0.5	3.6/0.5	1.5/1.0
	2	907/	938/	3.3/		
	3	1401/	1480/	5.3/		
	4	-	-	-		
3	1	403/671	400/669	-0.8/-0.3	2.7/0.4	1.5/1.0
	2	858/1345	865/1339	0.8/-0.4		
	3	1352/	1396/	3.2/		
	4	1811/	1888/	4.1/		
4	1	383/562	382/551	-0.3/-2.0	1.7/1.9	1.7/1.1
	2	791/1076	791/1054	0.0/-2.1		
	3	1268/1677	1289/1649	1.6/-1.7		
	4	1729/	1781/	2.9/		
5	1	386/658	388/635	0.5/-3.6	1.2/3.3	1.7/1.1
	2	749/1009	752/973	0.4/-3.7		
	3	1192/1516	1205/1469	1.1/-3.2		
	4	1648/2087	1682/2038	2.0/-2.4		

the same length and wall thickness. The physical properties of the shell material are as follows: Young' s modulus = 69.0 GPa, Poisson' s ratio = 0.3, and mass density = 2700 kg/m^3. Water is used as the contained fluid with a density of 1000 kg/m^3. The sound speed in water, 1483 m/s, is equivalent to the bulk modulus of elasticity, 2.2 GPa. Dimensions and material properties used for the analysis are shown in Table 1.

The frequency equation derived in the preceding section involves the double infinite series of algebraic terms. Before exploring the analytical method for obtaining the natural frequencies of the fluid-coupled shells, it is necessary to conduct convergence studies and establish the number of terms required in the series expansions involved. In the numerical calculation, the Fourier expansion term m is set at 100, which gives an exact enough solution by convergence. The coupled natural frequencies of the fluid-filled coaxial shells for the clamped boundary condition at both ends of two shells are shown in Table 2.

3.2. Finite Element Analysis

Finite element analyses using a commercial computer code ANSYS 5.5 [9] are performed to verify the analytical results for the theoretical study. The finite element method results are used as the baseline data. Three-dimensional model is constructed for the finite element analysis. The fluid region is divided into a number of identical 3-dimensional contained fluid elements (FLUID80) with eight nodes having three degrees of freedom at each node. The fluid element FLUID80 is particularly well suited for calculating hydrostatic pressures and fluid/solid interactions. The circular cylindrical shell is modeled as elastic shell elements (SHELL63) with four nodes. The model has 3840 (radially 4 x axially 20 x circumferentially 48) fluid elements and 1920 shell elements as shown in Figure 2.

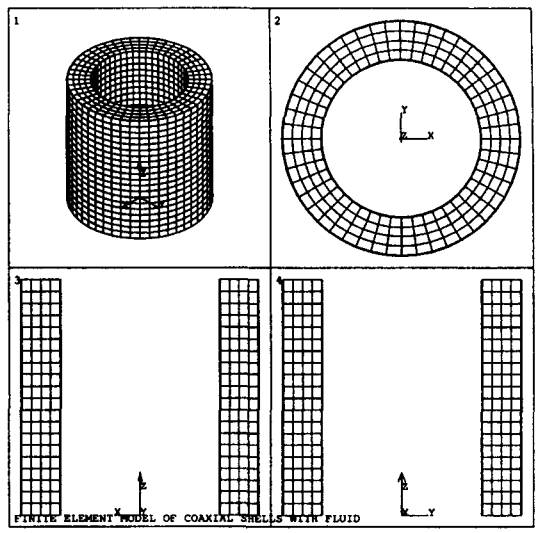

Fig. 2. Finite Element Model of Coaxial Cylindrical Shells with Fluid

The fluid boundary conditions at the top and bottom of the tank are zero displacement and rotations. The nodes connected entirely by the fluid elements are free to move arbitrarily in three-dimensional space, with the exception of those, which are restricted to motion in the bottom and top surfaces of the fluid cavity. The radial velocities of the fluid nodes along the wetted shell surfaces coincide with the corresponding velocities of the shells. For the shell, three boundary conditions are considered such as clamped-clamped, clamped-free and simply supported-simply supported conditions at both ends.

Sufficient number of master degree of freedoms is selected to calculate 200 frequencies and the reduced method is used for the eigenvalue and eigenvector extractions, which employ the Householder-Bisection-Inverse iteration extraction technique.

4. Results and Discussion

Mode shapes of the fluid-coupled coaxial shells

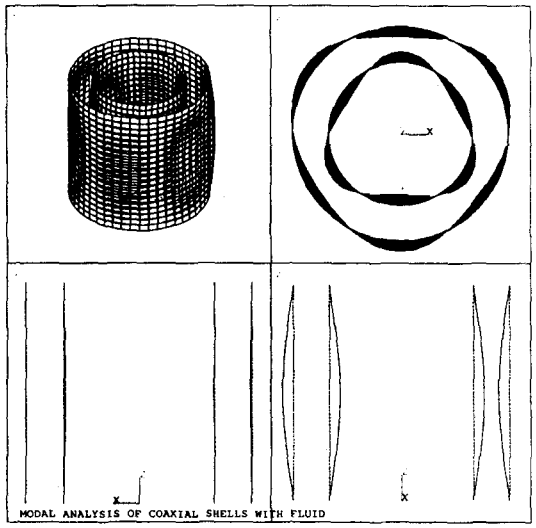

Fig. 3. Typical Mode Shape of Out-of-phase Mode (m' =1, n=3)

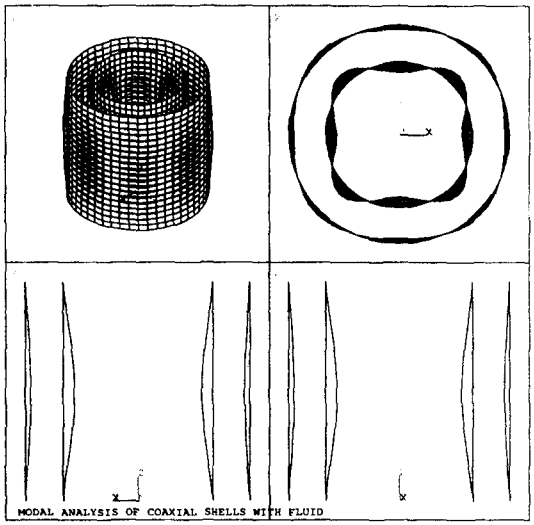

Fig. 4. Typical Mode Shape of In-phase Mode (m' =1, n=4)

are obtained by the finite element method and typical mode is plotted in Figure 3, which shows the deformed mode shape of the fluid and shell elements for the circumferential wavenumber n = 3. The dotted lines in the figures represent the undeformed shapes of the cylindrical shells.

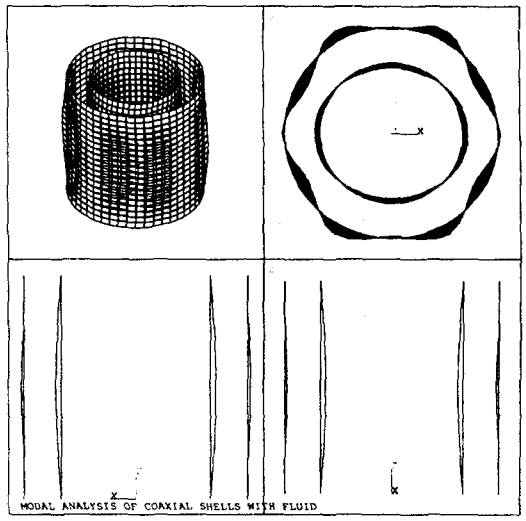

Fig. 5. Typical Mode Shape of Mixed Mode (m' =1, n=6 or 2)

The frequency comparisons between analytical solution developed here and finite element method are shown in Table 2 for the clamped boundary conditions at both ends. The discrepancy is defined as

$$\text{Discrepancy}(\%) = \frac{\text{frequency by FEM - theoretical frequency}}{\text{frequency by FEM}} \times 100 \,. \quad (31)$$

The largest discrepancies between the theoretical and FEM results are 7.4 % for the circumferential wave number, n=1 and 5.3 % for n=2. Discrepancies defined by equation (31) are always less than 8% with RMS value of 5.3% and crest factor of 1.7, therefore the theoretical results agree well with FEM results, verifying the validity of the analytical method developed.

All of the mode shapes can be classified into three mode categories according to the relative moving directions between the inner and outer shells during the vibration : in-phase mode (Figure 4), out-of-phase mode (Figure 3) and mixed mode (Figure 5). The vibrational mode shapes show some ambiguous vibrational modes, neither

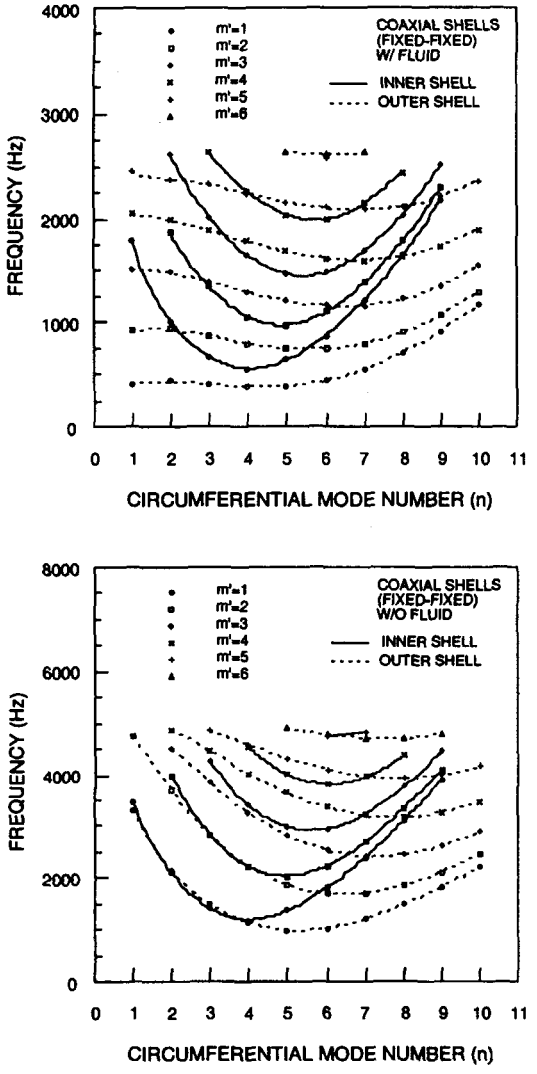

Fig. 6. Frequencies of Coaxial Shells for Clamped-Clamped Case

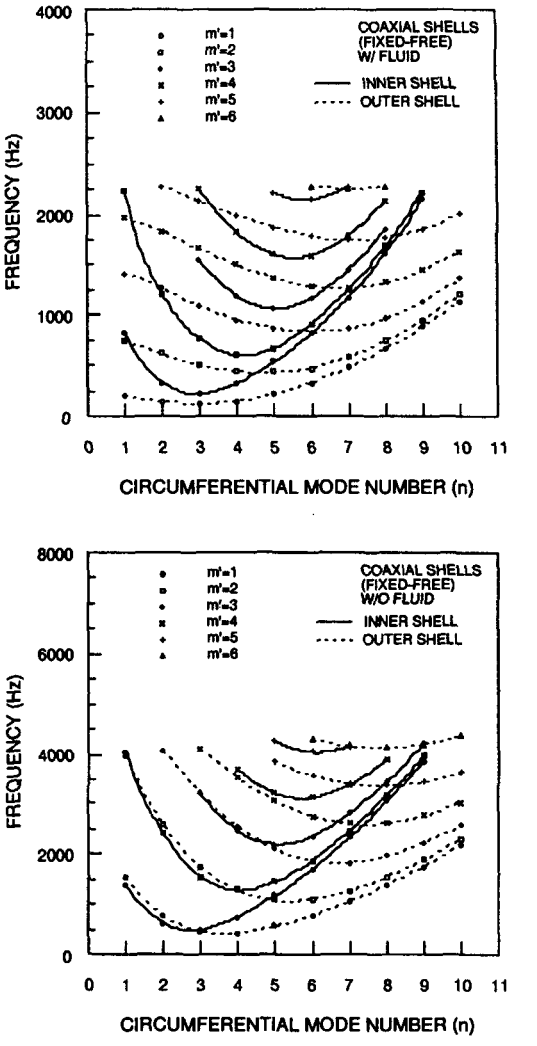

Fig. 7. Frequencies of Coaxial Shells for Clamped-Free Case

apparent in-phase modes nor apparent out-of-phase modes, which are called mixed vibrational modes. Reviewing the vibrational mode shapes revealed that as the axial mode number increases, the mixed vibrational modes appear frequently. As the circumferential mode number increases, the out-of-phase and in-phase modes in the serial vibrational modes appear alternatively.

The frequencies between coaxial shells with and without fluid-filled annulus are compared as shown in Figures 6 through 8 for different boundary conditions at both ends of the shell. In the case of shells without fluid-filled annulus, the inner and outer shells give almost the same frequencies for lower circumferential mode numbers, but as the circumferential mode number increases the frequencies of the inner shell were found to be

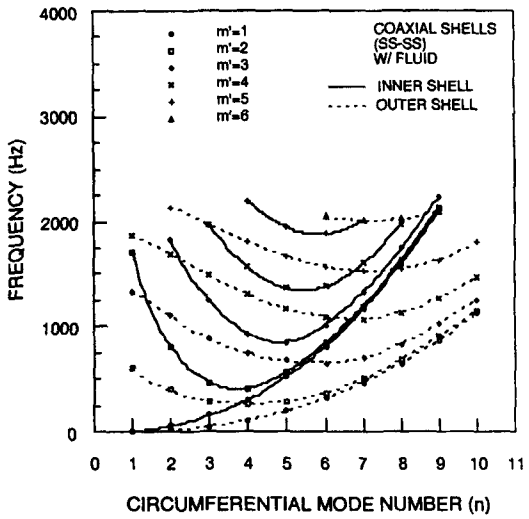

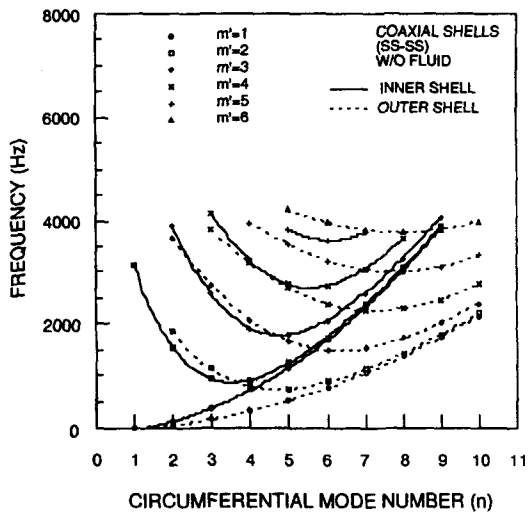

Fig. 8. Frequencies of Coaxial Shells for Simply Supported-Simply Supported Case

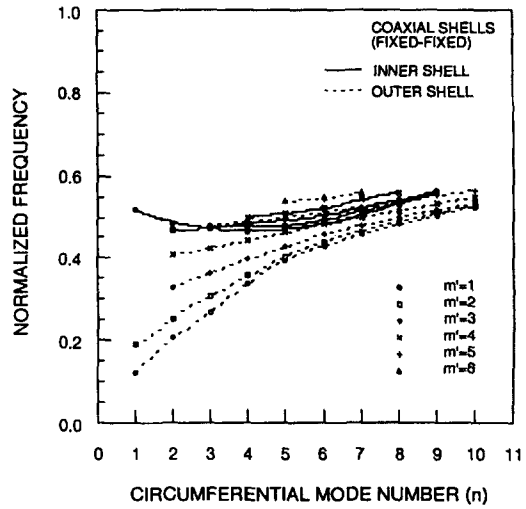

Fig. 9. Normalized Frequencies of Coaxial Shells (fixed-fixed case)

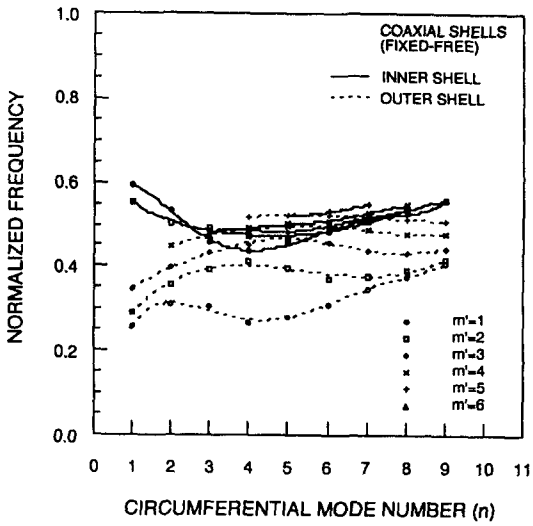

Fig. 10. Normalized Frequencies of Coaxial Shells (fixed-free case)

larger than those of outer shell frequencies. Contrary to this, for the case of shells with fluid-filled annulus, the frequencies of the inner shell are always higher than those of outer shell as the frequency deviates its lowest point. All three cases of different boundary conditions have the same trend.

The effect of fluid-filled annulus on the frequencies can be assessed using the normalized frequency defined as

$$\text{Normalized frequency} = \frac{\text{Frequency with fluid - filled annulus}}{\text{Frequency without fluid - filled annulus}}. \quad (32)$$

Figures 9 through 11 show the normalized

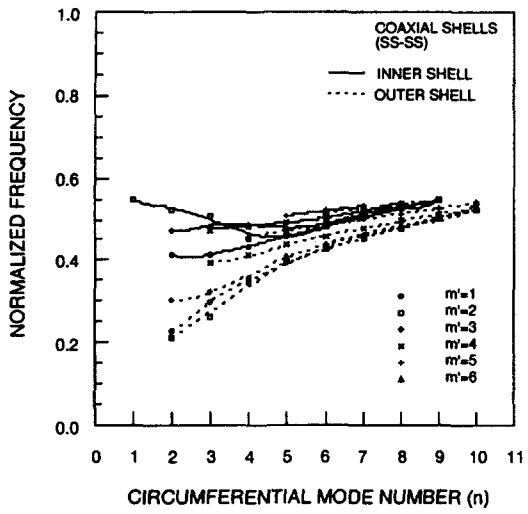

Fig. 11. Normalized Frequencies of Coaxial Shells (simply supported- simply supported case)

natural frequencies for three different boundary conditions. The reduction of the frequencies due to the inclusion of fluid-filled annulus is almost the same for the different boundary conditions. The frequencies of the outer shell decreases more than those of inner shell and the reduction rate ranges from 0.4 to 0.6 for the inner shell and from 0.1 to 0.6 for the outer shell. Also the lower circumferential modes are more affected by the inclusion of the fluid-filled annulus for the outer shell, but the inner shell has almost the same reduction rate all through the circumferential modes.

5. Conclusions

An analytical method to estimate the coupled frequencies of the coaxial cylindrical shells filled with fluid in the annular gap is developed using the series expansion method based on the Fourier transformation. To verify the validity of the analytical method developed, finite element method is used and the frequency comparisons between them are found to be in good agreement. The effect of fluid-filled annulus on the frequencies is investigated using a finite element method generating following conclusions ;

1) The reduction rate of the frequencies due to the inclusions of the fluid-filled annulus is almost the same for all boundary conditions.
2) The inclusion of fluid-filled annulus affects the outer shell more than the inner shell.
3) The frequencies of the shells with fluid-filled annulus decrease to 0.4 ~ 0.6 and 0.1 ~ 0.6 of those of shells in air for the inner and the outer shells, respectively.
4) For the case of outer shell, fluid-filled annulus effect is more significant for the lower circumferential modes.

References

1. Song, S.H., Jhung, M.J., 1999, "Experimental modal analysis on the core support barrel of reactor internals using a scale model," *KSME International Journal*, Vol.13, No.8, pp.585-594.
2. Jhung, M.J., 1996, "Shell response of core barrel for tributary pipe break," *International Journal of Pressure Vessels and Piping*, Vol.69, No.2, pp.175-183.
3. Chen, S.S., Rosenberg, G.S., 1975, "Dynamics of a coupled shell-fluid system," *Nuclear Engineering and Design*, Vol.32, pp.302-310.
4. Yoshikawa, S., Williams, E.G., Washburn, K.B., 1994, "Vibration of two concentric submerged cylindrical shells coupled by the entrained fluid," *Journal of Acoustic Society of America*, Vol.95, pp.3273-3286.
5. Fritz, R.J., 1972, "The effects of liquids on the dynamic motions of immersed solids," *Journal of Engineering for Industry*, Vol.94, pp.167-173.

6. Jhung, M.J., 1996, "Hydrodynamic effects on dynamic response of reactor internals," *International Journal of Pressure Vessels and Piping*, Vol.69, No.1, pp.65-74.
7. Jeong, K.H., Lee, S.C, 1996, "Fourier series expansion method for free vibration analysis of either a partially liquid-filled or a partially liquid-surrounded circular cylindrical shell," *Computers and Structures*, Vol.58, pp.937-946.
8. Sneddon, I.N., 1951, *Fourier Transforms*, McGraw-Hill Book, New York.
9. ANSYS, 1998, *ANSYS Structural Analysis Guide*, ANSYS, Inc., Houston.